JOURNAL OF THE AMERICAN WATER RESOURCES ASSOCIATION
AUGUST AMERICAN WATER RESOURCES ASSOCIATION 2006

CUMULATIVE EFFECTIVE STREAM POWER AND BANK EROSION ON THE SACRAMENTO RIVER, CALIFORNIA, USA[1]

Eric W. Larsen, Alexander K. Fremier, and Steven E. Greco[2]

ABSTRACT: Bank erosion along a river channel determines the pattern of channel migration. Lateral channel migration in large alluvial rivers creates new floodplain land that is essential for riparian vegetation to get established. Migration also erodes existing riparian, agricultural, and urban lands, sometimes damaging human infrastructure (e.g., scouring bridge foundations and endangering pumping facilities) in the process. Understanding what controls the rate of bank erosion and associated point bar deposition is necessary to manage large alluvial rivers effectively. In this study, bank erosion was proportionally related to the magnitude of stream power. Linear regressions were used to correlate the cumulative stream power, above a lower flow threshold, with rates of bank erosion at 13 sites on the middle Sacramento River in California. Two forms of data were used: aerial photography and field data. Each analysis showed that bank erosion and cumulative effective stream power were significantly correlated and that a lower flow threshold improves the statistical relationship in this system. These correlations demonstrate that land managers and others can relate rates of bank erosion to the daily flow rates of a river. Such relationships can provide information concerning ecological restoration of floodplains related to channel migration rates as well as planning that requires knowledge of the relationship between flow rates and bank erosion rates.
(KEY TERMS: bank erosion rates; fluvial processes; meander migration; rivers/streams; stream power; surface water.)

Larsen, Eric W., Alexander K. Fremier, and Steven E. Greco, 2006. Cumulative Effective Stream Power and Bank Erosion on the Sacramento River, California, USA. Journal of the American Water Resources Association (JAWRA) 42(4):1077-1097.

INTRODUCTION

Natural rivers and their surrounding areas constitute some of the world's most diverse, dynamic, and complex terrestrial ecosystems (Naiman *et al.,* 1993). Land deposition on the inside bank of a curved river channel is a process that creates opportunities for vegetation to colonize the riparian corridor (Hupp and Osterkamp, 1996; Mahoney and Rood, 1998). Point bar deposition and outside bank erosion are tightly coupled. These physical processes (which constitute channel migration) maintain ecosystem heterogeneity in floodplains over space and time (Malanson, 1993). Channel migration structures and sustains riparian landscapes that in turn provide essential habitat for many species of concern (Tabacchi *et al.,* 1998). At the same time, river channel bank erosion can be detrimental to human structures and adjacent lands. On many large alluvial rivers, engineering efforts have focused on restraining bank erosion to protect physical structures (bridges and roads), parts of cities, and private lands. But bank hardening (riprap) and near-bank levees can have significant effects on fluvial processes such as lateral channel migration and chute cutoffs. These events help establish new riparian communities, promote their survival, and form ecologically important oxbow lakes (Gergel *et al.,* 2002).

Increasingly, resource managers recognize that the natural migration of river channels can conserve and restore ecosystem processes (Golet *et al.,* 2003). River channel managers can benefit from understanding the processes and patterns of river bank erosion.

[1]Paper No. 04232 of the *Journal of the American Water Resources Association* (JAWRA) (Copyright © 2006). **Discussions are open until February 1, 2007.**

[2]Respectively, Associate Research Scientist, Student, and Assistant Professor, Department of Environmental Design, University of California-Davis, One Shields Avenue, Davis, California 95616 (E-Mail/Larsen: ewlarsen@ucdavis.edu).

Within alluvial river systems, bank retreat and channel migration are caused by bank erosion and associated point bar building. These processes occur at rates that vary at every location along the river reach. Bank erosion involves a variety of processes, including fluvial entrainment and bank mass failure (ASCE, 1998; Darby and Thorne, 1996; Osman and Thorne, 1988; Pizzuto and Meckelenburg, 1989). Physical factors that determine bank erosion include local curvature, sediment composition of banks, bank geometry (including height), in-stream sediment transport, and flow magnitude near banks (ASCE, 1998). Hasegawa (1989) gives an analytical expression for a "universal [bank] erosion coefficient" as a function of (1) flow velocity, (2) change in bed elevation, (3) near bank velocity, (4) relative depth of bed scour, (5) relative bank height, and (6) cross stream near bottom flow velocity. From scaling arguments, he suggests that near bank velocity and relative bank height are the most important factors. Similarly, Hickin and Nanson (1984) suggest that bank migration is a function of at least five variables including unit stream power (the stream power per unit width of channel), opposing force per unit boundary area resisting migration, bank height, bend radius, and channel width. Hickin and Nanson (1984) and Nanson and Hickin (1986) applied this concept to 18 meandering river channels in Western Canada. Their research indicated that erosion rate is a function of unit stream power, outer bank height, and a coefficient of resistance to lateral migration. Of the factors that influence bank erosion, flow magnitude may be the most important. Knighton (1998) acknowledged the synergy of actions that generate bank erosion, but concluded that hydraulic action caused by near-bank velocities is of major importance.

This paper investigates the relationship between the flow component and bank erosion rates. It addresses whether there is an empirical correlation between the sum of stream power and the amount of bank erosion in different time intervals. Two datasets are used: one based on aerial photography and the other on field data. Other variables that affect bank erosion rates are not accounted for in these empirical relationships and therefore will be captured within the residuals (unexplained variation) in the results. The influence of many of these other variables can be better accommodated by specifically modeling the link between channel curvature and channel migration as well as other variables (e.g., Johannesson and Parker, 1989). This study is therefore empirical in nature, but its results can be used in mechanistic models to help predict bank migration. Moreover, the relationship can help to correlate historical patterns of migration to successional patterns of vegetation and habitat change over time (e.g., Richter and Richter, 2000). This model can improve the management of large floodplain rivers, including quantifying environmental benefits of flow prescriptions by projecting floodplain dynamics in relation to specific flow alterations. This application is explored in a companion paper (Larsen *et al.,* 2006a) based on the results presented here.

METHODS

Study Sites and Data Sets

The Sacramento River (Figure 1) is the largest river in the state of California and drains an area of 2,305,100 ha (CALWATER, 1997). Collecting precipitation and snowmelt runoff from the western slopes of the Sierra Nevada, the eastern slopes of the Coast Range, and the southern Trinity and Klamath ranges, the river drains 17 percent of the land in California. The river flows from north to south, with a length of about 483 km. Its waters flow though San Francisco Bay and enter the Pacific Ocean. For more details on hydrology see the companion paper (Larsen *et al.,* 2006a).

Various systems to reference the length of the Sacramento River have been used, the most common being a set of "river mile" (RM) markers established by the U.S. Army Corps of Engineers (USACE) in 1964. According to this measuring system, the river extends from the confluence of the Sacramento and San Joaquin rivers (RM 0) at the San Francisco Bay to near Shasta Dam (about RM 312) (Figure 1).

Channel constraints have been installed in almost the entire lower half of the Sacramento River (upstream to the town of Colusa at RM 143). Only the upper half, from Colusa to Red Bluff (RM 143-244), is a freely meandering reach. However, riprap also exists along the banks of much of this reach.

The Sacramento River between Red Bluff and Colusa is primarily a single-thread sinuous channel (Figure 1). The two-year recurrence interval is approximately 2,270 m^3/s. The slope, averaged over a minimum of 5 km, ranges from 0.0002 m/m to 0.0007 m/m (Water Engineering and Technology, Inc., 1988). The riverbed material is primarily sand and pebbly gravel with a median grain size that ranges from 20 to 30 mm in the reach RM 196 to199 (Water Engineering and Technology Inc., 1988). The channel banks are composed of sand and gravel with isolated patches of erosion-resistant rock types (CDWR, 1995). Between RM 196 and RM 199, the average (mean) bank height from thalweg to top of the bank is about 6 m, and ranges from 2 to 8 m. The mean diameter of

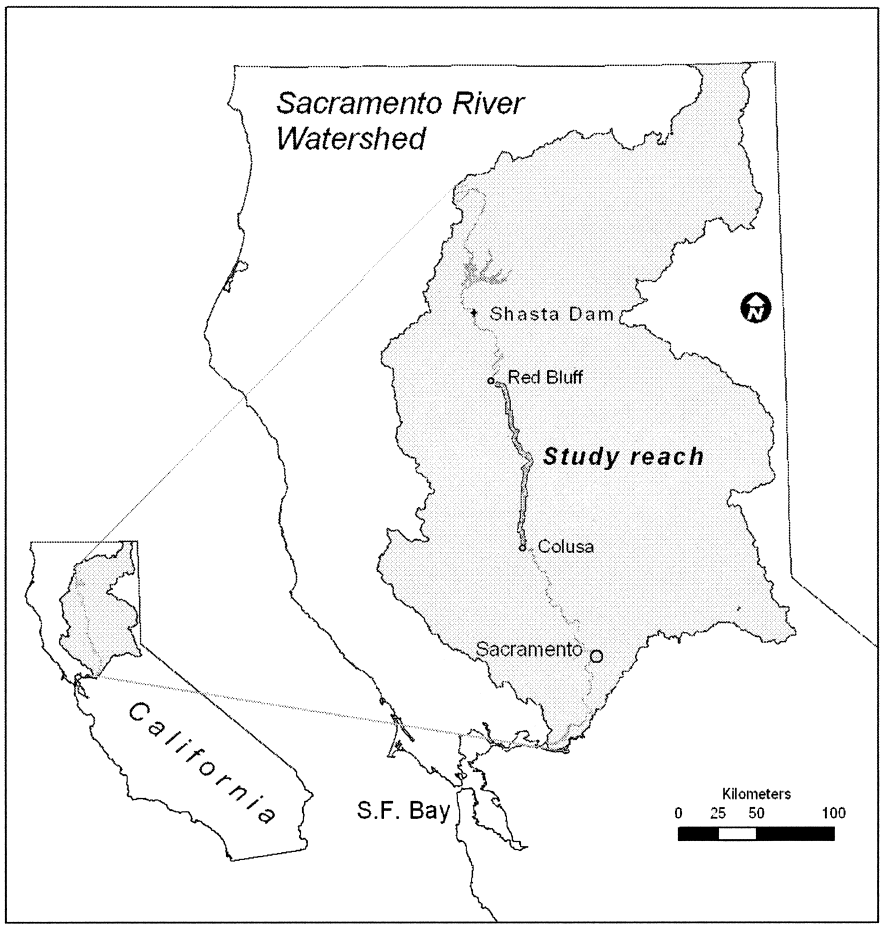

Figure 1. Site Location Map of the Meandering Reach of the Sacramento River, California, USA.

the gravel in the eroding banks in the vicinity of this site is 8 mm and ranges from 4 mm to 11mm (CDWR, 1995).

Two different types of data were used in this study to measure changes in channel bank locations (i.e., bank erosion). The first dataset is based on a detailed study of channel migration near Pine Creek Bend, at RM 196.5 (Figure 2) using a time sequence of aerial photography. The second dataset is a series of bank erosion measurements surveyed in the field at 12 sites along the middle Sacramento River by the California Department of Water Resources (CDWR) (Figure 2). These study sites were located at areas on the river where extensive bank erosion data were collected between 1988 and 2001 by the CDWR (e.g., Figure 3).

The Pine Creek site was selected for analysis because of its channel migration history and the availability of a set of aerial photographs ranging in scale from 1:6,000 to 1:20,000 representing 13 time periods from 1937 to 1975 (Fremier, 2003; Greco *et al.,* 2003). The 1937 photographs are the earliest known aerial photos taken at the Pine Creek site; photos after 1975 were not used because the cutbank edge of the bend was hardened with rock revetment (riprap) that year and migration was essentially halted.

From the rectified aerial photos at the Pine Creek site, planform maps showing channel locations were digitized into a geographic information system (GIS) database. For a detailed description of the channel mapping process, see Greco and Plant (2003) and Greco and Alford (2003). Channel bank lines were mapped on clear acetate layered over the aerial photographs, scanned, vectorized, and projected into real world coordinates using ArcGIS tools (ESRI, 2003). Control points were derived from U.S. Geological Survey (USGS) orthophoto quadrangles. From these georeferenced line files, polygons were generated for each river channel within the study reach. Erosion area and channel length were calculated from these data.

The second data set consisted of bank erosion measurements conducted by the Northern District of the CDWR at 12 sites on the river within the freely meandering sector (Figure 2). Cutbanks were surveyed at uneven time intervals from 1986 to 2001. Before 1996, surveys at each site were made using either a survey instrument or a total station across the river from the eroding cutbank. Angles ranging from 1 to 5 degrees were measured from a fixed back sight, and distances

were measured using an electronic laser distance meter. Bank measurements were accurate to approximately 1.5 m (CDWR, 1994). After 1996, cutbanks were measured by walking along the edge of the eroding bank with a global positioning system (GPS) antenna on the end of a ranging rod. CDWR used a Pathfinder GPS with post-processing data correction (submeter accuracy). To document bank erosion rates, the distances were resurveyed approximately semiannually up through 1993 and at various time intervals since then (example site shown in Figure 3). Points were input into AutoCAD (AutoDesk, 2004), georeferenced, and lines between points were interpolated to create an approximate cutbank arc. Results from field surveys through 1993 (CDWR, 1994) showed that annual bank erosion rates at the sites were highly variable but averaged about 2.5 m per year for this period. Higher migration rates were attributed to less cohesive bank material due to higher sand composition (K. Buer, CDWR, 2004, personal communication). The field measurement derived cutbank files were imported into ArcGIS to facilitate the present analysis and allow comparisons to the aerial photo derived GIS datasets.

Bank Erosion Rates

The area eroded between photo years was calculated based on the georeferenced channel maps for the Pine Creek site and cutbank maps for the CDWR erosion sites. The two datasets differ slightly; at the Pine Creek site, maps encompassed two bends, while all other sites contained only one. In the aerial photos, channel position was represented as a polygon of the entire channel, whereas the CDWR dataset represented the cutbank position as a line. To account for variable channel length, the area eroded was measured and then normalized by the average reach length between time intervals, resulting in a mean bank migration per unit length of channel (Larsen *et al.,* 2002, Micheli *et al.,* 2004). Reach length was calculated from the centerlines of each channel for the Pine Creek data, and the cutbank length for the CDWR dataset. The average bank erosion for the regression models is expressed as a distance in meters [i.e., area eroded (m^2) / average reach length (m)]. This value is often expressed as a function of time (m/yr).

The methods of calculating the area eroded between time intervals were similar in both datasets. For the aerial photo dataset (Pine Creek), the procedure was modified from a floodplain age model by Fremier (2003) to quantify the area eroded rather than the area deposited. No channel cutoff events occurred at any of the sites during the study periods.

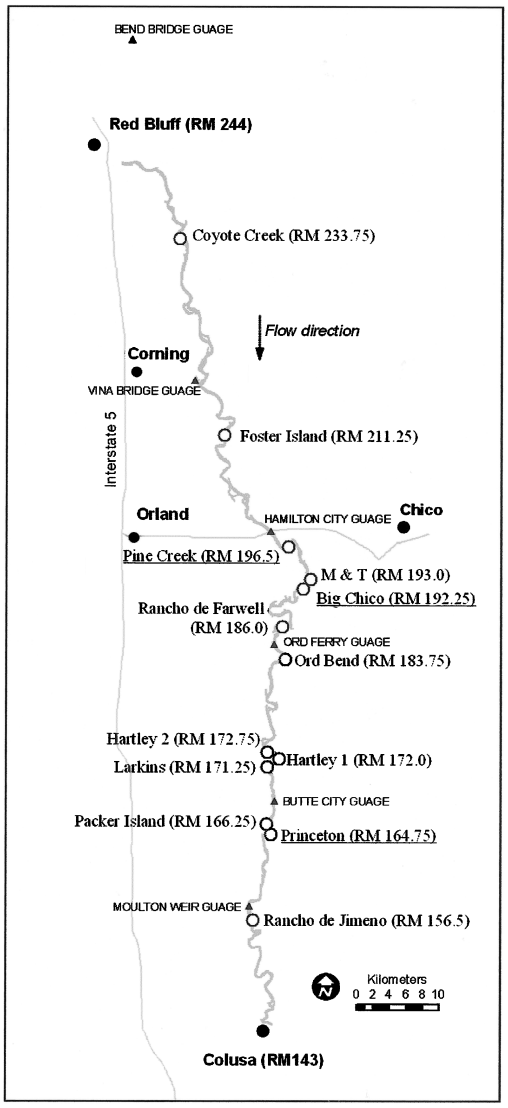

Figure 2. Study Site Locations Along the Sacramento River. These include 12 bank erosion sites and one site measuring bank retreat using aerial photography (Pine Creek RM 196.5). Numbers following site names refer to the "River Mile."

Cumulative Effective Stream Power

In cases where hydraulic forces alter the stream (processes ranging from sediment transport to bed rock river formation), researchers have used stream power to represent the forces moving sediment (e.g., Begin, 1981; Hickin and Nanson, 1984; Leopold *et al.,* 1964; Sklar and Dietrich, 2004). Leopold *et al.* (1964), based on the work of Bagnold (1960), argue from a mechanical standpoint that stream power represents "the rate of doing work ... by the flowing water." Available stream power, as defined by Leopold *et al.* (1964, p. 178) is

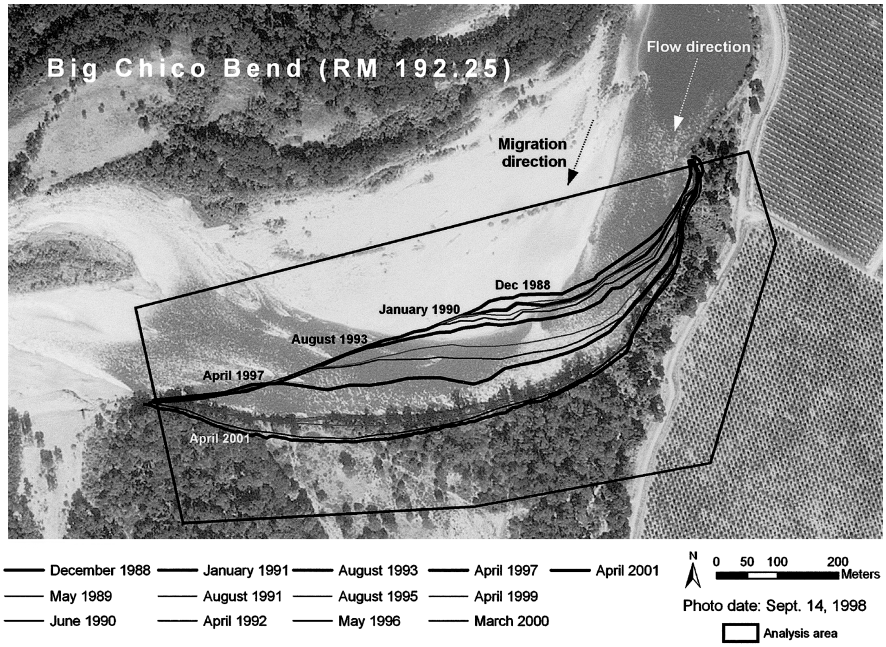

Figure 3. Bank Erosion Site – Big Chico Bend. The bank lines show surveyed location of the bank in different years (CDWR, 1995).

$$\Omega = \gamma QS \quad (1)$$

Stream power (Ω, kg m/s^3) is a rate of potential energy expenditure per unit length of channel, calculated as the product of discharge (Q, m^3/s), slope (S, m/m), and the specific weight of water (γ, kg/m^{2}s^2). Equation (1) can be manipulated to express stream power as the product of bed shear stress times the mean streamwise velocity multiplied by width

$$\Omega = \tau\, u\, w \quad (2)$$

where τ (kg/ms^2) is the bed shear stress, u (m/s) is the velocity, and w (m) is the width of the channel. In this form, stream power is represented as a force (bed shear stress) times a velocity times a scale of the channel size (width).

Stream power (used as a surrogate for the sum of the flow forces acting on a specific reach of stream bank over a designated time period) was related to bank erosion rates. Stream power was calculated from surface streamflow records collected at various sites along the Sacramento River by the USGS. Daily mean streamflow was obtained from the USGS (USGS, 2004) at gauging sites closest to each study reach (Table 1, Figure 2). For the Pine Creek dataset, the Bend Bridge Gauge (No. 11377100) was used because it was the only gauge with continuous records over the longer time period (1937 to present). Flows for that period of time ranged from a mean daily maximum of 7,400 m^3/s in 1937, to a mean daily low of 57 m^3/s in 1944. Cumulative annual discharge for the period of record is shown in Figure 4.

Threshold Values

A threshold discharge ($Q_{\text{lower threshold}}$) below which erosion is negligible was assumed and tested. The assumption of an upper threshold discharge ($Q_{\text{top of bank}}$) where the water flowing out of the channel theoretically no longer exerts force on the bank itself (Figure 5) was also tested. Therefore, for each site, the instantaneous effective stream power (Ω_e) was calculated as

$$\Omega_e = 0 \qquad \text{if } Q \le Q_{\text{lower threshold}}, \quad (3a)$$

$$\Omega_e = \gamma SQ - \gamma SQ_{\text{lower threshold}} \qquad \text{if } Q_{\text{lower threshold}} < Q < Q_{\text{top of bank}} \quad (3b)$$

$$\Omega_e = \gamma SQ_{\text{top of bank}} - \gamma SQ_{\text{lower threshold}} \qquad \text{if } Q \ge Q_{\text{top of bank}} \quad (3c)$$

where Q (m^3/s) is the mean daily flow rate at the site, estimated from available gauging records, and S is water surface slope. The *cumulative* effective stream power (Ω_{ce}) was then calculated by summing over the seconds in each measurement time interval

$$\Omega_{ce} = \sum \Omega_e \quad (4)$$

The hypothesis was made that the relationship between erosion and stream power is valid only between a specific range of discharges (Figure 5). A simple linear regression was used to estimate the 'lower threshold' of this range. To identify the 'best

TABLE 1. Bank Erosion and Aerial Photography Study Site Descriptions. The column "River Mile" gives the river mile as given in the USACOE method. "River Gauge" identifies the gauging station used for the discharge information at this site. Slope and $Q_{top\ of\ bank}$ were calculated in HEC-RAS for each bend.

Site	River Mile	River Gauge (RM)	Slope (S)	$Q_{top\ of\ bank}$ (m^3/s / ft^3/s)
Coyote Creek	233.75	Bend Bridge (258)	0.0002	2,300 / 80,000
Foster Island	211.75	Vina (218)	0.0002	2,300 / 80,000
Pine Creek	196.50	Bend Bridge (258)	0.0002	2,300 / 80,000
M & T	193.00	Hamilton City (199)	0.0004	2,800 / 100,000
Big Chico	192.50	Hamilton City	0.0003	2,800 / 100,000
Rancho de Farwell	186.00	Ord Ferry (184)	0.0007	3,000 / 110,000
Ord Bend	183.75	Ord Ferry	0.0007	3,000 / 110,000
Hartley 1	173.50	Butte City (169)	0.0003	3,000 / 110,000
Hartley 2	172.75	Butte City	0.0003	3,000 / 110,000
Larkins	171.25	Butte City	0.0003	3,000 / 110,000
Packer Island	167.00	Butte City	0.0001	2,300 / 80,000
Princeton	164.75	Butte City	0.0002	2,300 / 80,000
Rancho de Jimeno	156.50	Moulton Weir (158)	0.00015	2,600 / 90,000

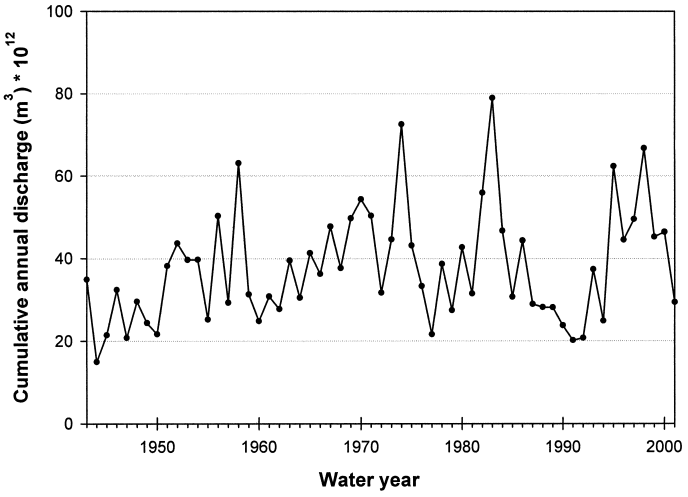

Figure 4. Cumulative Annual Discharge (m^3) From 1944 to 2002 at the Bend Bridge Gage.

lower threshold,' a range of potential values was tested. The estimated values do not necessarily represent a specific physical characteristic or process but are instead a statistical measure of a discharge below which the accumulated flows do not cause significant bank erosion. The increment of bank erosion (distance eroded per unit length of the reach) was plotted against cumulative effective stream power in the same time interval using lower-threshold discharge values ranging from 0 to 1,700 m^3/s. The largest discharge tested (i.e., 1,700 m^3/s) included previous estimates of a lower threshold for bank erosion (Buer *et al.*, 1989).

Regression relationships between bank erosion and stream power were performed for a range of lower threshold values. The coefficient of determination (r-squared) was used to determine which lower threshold gave the best relationship. From the many individual graphs of stream power versus erosion, the

$$\Omega_{ce} = \gamma Q_{ce} S \quad where \quad Q_{ce} = \sum_{Time1}^{Time2} Q_{effective}$$

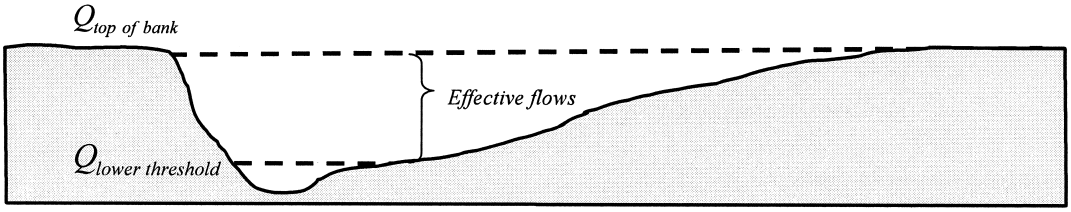

Figure 5. Effective Stream Power is Measured as the Discharge That Flows Between Lower and Upper Thresholds. Cumulative effective stream power (Ω_{ce}) is calculated by summing all daily values of effective stream power. Stream power is the product of the reach slope (S), the specific weight of water (γ) and discharge (Q).

r-squared value, the p-value, and the number of nonzero values of each relationship were recorded. Zero values of effective stream power occurred when the lower threshold was not exceeded in a given time period.

More sophisticated statistical methods were considered as an alternative to simple linear regression; however, linear regression was chosen because it revealed patterns readily and is widely understood and practiced. In the pooled data analysis (of all sites), the data were log-transformed. In the plotted relationships between lower-threshold discharge and r-squared value, the curve was examined beyond the maximum point to determine if there was a distinct maximum or if there was a plateau or asymptote at or near the maximum. This procedure produced a best estimate of the discharge at which significant migration is initiated (i.e., Q_{lower} threshold).

The upper threshold ($Q_{top\ of\ bank}$) represents the hypothetical discharge at which water flowing out of the channel would no longer exert significant additional force on the bank. Discharges exceeding the top of the bank value were assumed to exert the same forces on the bank as flows just reaching the top of the bank. On the middle Sacramento River, the channel floodplain is rarely confined; overbank flows spread out in a shallow and slow moving flow over broad floodplains. For this study, a HEC-RAS hydrologic model was used to determine the top of bank discharge and energy grade line at each site (USACE, 2002). The energy grade line represents the water surface slope at the top of bank discharge. The slope was not varied according to stage discharge relationships. From the cross sections available, the "top of the bank" was estimated to be where the water spilled over the cutbank into the floodplain. The discharge (Q) that would fill the channel to the estimated top of bank was then modeled with HEC-RAS. Site specific estimates were checked by modeling the same flow through cross sections one-quarter mile upstream and downstream from the site. Cross section shape differed only slightly at adjacent sections, and therefore served as a qualitative check on the magnitude of top-of-bank flow magnitude.

Study Sites and Grouping of Data Sets

Sites were analyzed individually and grouped. Statistical limitations disqualified some sites from the individual site analysis step; however, all sites were included in the group analysis. The statistical limitations with the data involved the timing of the bank erosion field measurements. Ten sites had an uneven distribution of data points over time, causing some data points to exert a disproportionate effect on the regression (i.e., statistical leverage points). Cutbank location data were collected roughly every six months during dry years, when stream power values – and thus migration rates – were very low. In addition, data were not collected for many years when the channel moved significantly due to high flow discharges. This caused the 10 datasets to have many very small values and a few very large ones, but few middle values.

Three sites were selected for individual analysis, each consisting of a short length of river (one to two bends). The data from these sites were analyzed to correlate Ω_{ce} and bank erosion at an individual site. At this scale, other variables, such as bank material and bank height, are presumably relatively constant. For this reason, it was hypothesized that the relationship between flow (Ω_{ce}) and channel migration would likely be more precise at the site level.

The sites were then analyzed as a group to show relationships among multiple sites or at larger reach scales. Two groups of sites were investigated: the three sites used in the site analysis, and all of the sites. Initially, all data points were included (even previously described leverage points) because large values at the site level were not uniquely large when the data were pooled. In addition, points with a migration distance (area eroded divided by reach length) less than one meter were not used in the analysis because they were smaller than the minimum mapping unit (less than the error of data collection). Afterwards, only sites with a sample size greater than seven points were used to test the threshold values for the detailed study. A goodness-of-fit test [Shapiro-Wilk (W)] was performed to test the normality assumption of linear regression. The data (Appendix A) were analyzed with a linear and log-log relationship (for the combined analysis only).

RESULTS

Migration Rates

Mean annual erosion rates ranged from 0.4 m/yr at the M&T site with six years of record to 8.9 m/yr at Pine Creek with 18 years of record (Table 2). The mean annual erosion rate for the 13 sites was 3.7 ± 1.7 meters per water year. On average, the fastest migrating sites were Pine Creek, Big Chico, and Princeton. The relationship between the radius of curvature and migration rate for the 13 sites shows a pattern similar to that first noted by Hickin and Nanson (1984): migration rates are the highest on bends having a radius of curvature between two and three

TABLE 2. Erosion Characteristics at Each Study Site. Calculated average, maximum, and minimum bank erosion rates per site. Time intervals for each metric indicate when the values where measured.

Bend Name	Radius of Curvature (R/W*)	Bank Toe D_{84} (mm)	Mean Erosion Rate (m/year)	Begin Date	End Date	Maximum Erosion Rate (m/year)	Begin Date	End Date	Minimum Erosion Rate (m/year)	Begin Date	End Date
Coyote Creek	4.3	45	1.2	6/15/1988	5/15/2000	4.0	8/15/1993	5/15/2000	0.02	1/15/1991	6/15/1991
Foster Island	6.9	13	1.8	6/15/1988	4/15/2001	7.9	8/15/1993	6/15/2000	0.00	7/15/1991	5/15/1992
Pine Creek	2.8	0.4	8.9	9/7/1937	5/27/1975	16.5	6/7/1968	5/20/1970	2.6	6/13/1947	7/18/1951
M & T	7.9	0.4	0.4	5/15/1995	4/15/2001	1.5	6/15/1999	8/15/1999	0.00	5/15/1997	6/15/1999
Big Chico	2.9	0.4	7.0	6/15/1988	4/15/2001	19.0	4/15/1997	4/15/1999	0.2	5/15/1989	6/15/1990
Rancho de Farwell	2.0	7	2.9	8/15/1986	4/15/2001	13.7	6/15/1990	1/15/1991	0.0	8/15/1986	1/15/1987
Ord Bend	2.8	23	1.7	8/15/1986	4/15/2001	7.7	11/15/1992	11/15/1993	0.0	8/15/1986	1/15/1987
Hartley 1	2.5	15	4.2	8/15/1986	5/15/2001	27.3	11/5/1992	8/15/1993	0.01	11/15/1986	5/15/1987
Hartley 2	3.7	15	1.4	6/15/1988	5/15/2001	5.4	12/15/1993	5/15/2001	0.00	1/15/1991	9/15/1991
Larkins	2.5	15	1.8	8/15/1986	5/15/2001	13.2	11/15/1992	8/15/1993	0.00	8/15/1986	11/15/1986
Packer Island	2.5	15	6.3	6/15/1988	5/15/2000	21.3	11/15/1992	8/15/1993	0.1	6/15/1989	6/15/1990
Princeton	2.0	15	8.0	11/15/1986	5/15/2001	38.8	11/15/1992	5/15/1995	0.00	6/15/1990	1/15/1991
Rancho de Jimeno	1.6	3	3.0	6/15/1988	5/15/2001	7.1	11/15/1992	6/15/2000	0.2	6/15/1989	6/15/1990
Average for All Sites	3.4	13	3.7	–	–	–	–	–	–	–	–

*w = 230 m.

channel widths (Figure 6). In this figure, the points are the Sacramento River data, and the line is based on data from the Beatton River in Canada (Hickin and Nanson, 1984).

Bank Erosion and Stream Power at Detailed Study Sites

Lower Threshold. When the r-squared value (coefficient of determination) was plotted against the lower discharge threshold, each of the graphs, except the one for all 13 datasets combined, had similarly shaped single-peak lines with a maximum r-squared value occurring between 310 and 400 m^3/s (Figure 7). Each individual regression, using lower threshold values ranging from 0 to 1,700 m^3/s, was statistically significant (alpha < 0.05). The "best lower threshold" and "no lower threshold" data sets were plotted against erosion (Figure 8, Table 3). These three regression plots have an even distribution of data points across the predictor variable (x-axis) with plus or minus eight points. The Pine Creek bend dataset covers a longer time period (38 years) than the field datasets, and has a lower r-squared value (Table 3). Lower thresholds for Pine Creek, Big Chico, and Princeton bends were 310, 340, and 400 m^3/s, respectively. The goodness-of-fit test (W) for the residuals at each site for both the nonthreshold and threshold models was not significant at the Pine Creek site ($W = 0.94$, $P < 0.47$ and $W = 0.95$, $P < 0.64$, respectively) and Big Chico Creek site ($W = 0.96$, $P < 0.82$ and $W = 0.94$, $P > 0.47$, respectively), while the Princeton site was significant ($W = 0.65$, $P < 0.001$ and $W = 0.65$, $P > 0.001$, respectively). A significant relationship shows that the residuals for this linear regression were not normally distributed.

Using Lower and No Lower Threshold. The relationship between bank erosion and stream power was compared using the best lower threshold and using no lower threshold (Figure 8 and Table 3). The fit line (a) on each graph shows the relationship when no lower discharge threshold was used. The r-squared values using the best lower threshold (b) are greater than the r-squared values using no lower threshold. Based on this, the relationship with the best lower threshold was used. In the regression relationships in Figure 8, the slopes (i.e., rate of erosion per unit stream power) of the two lines (with and without a lower threshold) differ. The use of a lower threshold produces a higher rate of erosion (steeper slope) because flows below the lower threshold were removed. Removing flow

from the cumulative stream power increases the calculated rate of erosion per unit flow. Slopes of the regression lines at all three sites, using a lower threshold, are similar, varying from 4.9 to 6.0 (x 10^{-11}). The differences in relationship results are most likely the result of other physical factors such as bank erodibility, channel width, and bank height. None of these is accounted for when comparing sites. The channels at all three sites have a relatively similar radius of curvature to width ratio (r/w) of 2 to 3, and therefore have relatively similar curvatures.

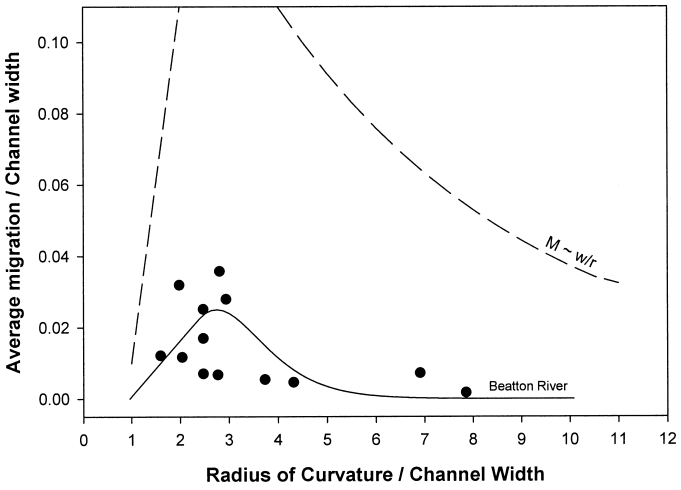

Figure 6. Radius of Curvature and Migration Rates (standardized by channel widths). The Sacramento River data (points) are plotted along with the two curves taken from Hickin and Nanson (1984). The lower curve is a curve that was originally fit to data from Beatton River and the upper curve represents an upper limit of 21 rivers surveyed in Western Canada.

Upper Threshold. Regression relationships between stream power and bank erosion were calculated twice, once including and once excluding discharges that exceeded the top-of-bank threshold. The r-square value was essentially the same for both analyses (Table 3, lines b and c). Our final results do not take into account an upper threshold, and therefore the sum of all overbank flows in the cumulative effective stream power was included.

Bank Erosion and Stream Power at Multiple Sites

We combined the data from the three sites used for individual analysis and analyzed the results (Figures 7 and 9, and Table 3). The r-squared values ranged from a low of below 0.70 to a high of 0.85 (Figure 7). The ordinate values rose monotonically to the maximum value and declined as lower discharge thresholds increased (abscissa values). This trend is similar to that found for the three individually analyzed study sites.

Finally, all 13 datasets were combined to analyze the relationship between cumulative effective stream power and bank erosion. The same statistical procedure was performed to identify the lower threshold. Figure 7 shows how the r-squared value changes when the lower threshold is increased. The best relationship was found to be at 430 m^3/s, although it has neither a clear maximum nor greatly differs from the regression without a lower threshold (r-squared = 0.70 and 0.71, respectively). The slopes of the lines were 1.3 x10^{-11} without a threshold and 2.5 x10^{-11} with a lower threshold (Figure 9 and Table 3). It is

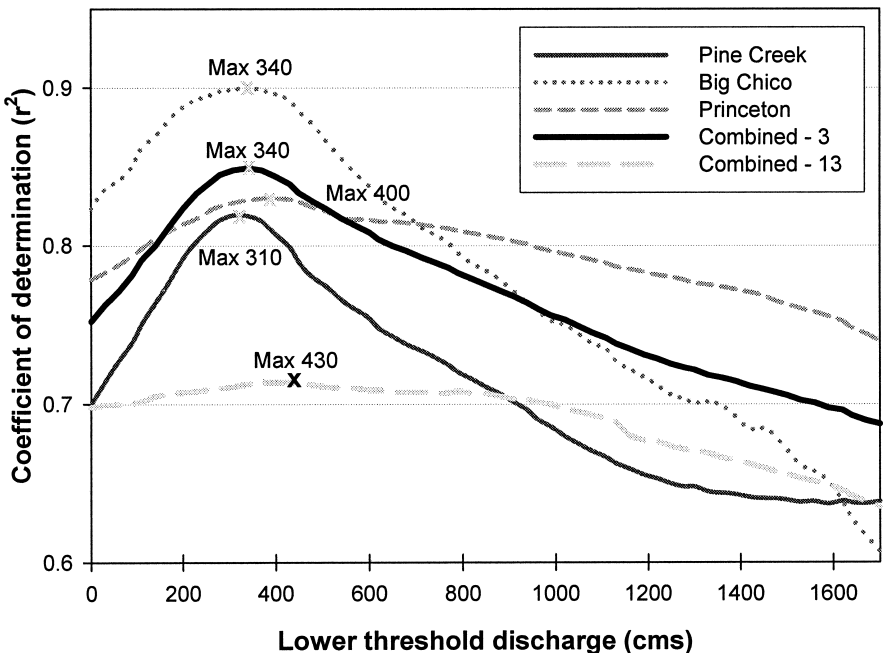

Figure 7. R-Squared Values of the Regression of Erosion (migration distance) Onto Ω_{ce} for All Analyses. The curve shows the response in r-squared values when changing the lower threshold for each individual site (three), these three sites combined, and all sites combined (13).

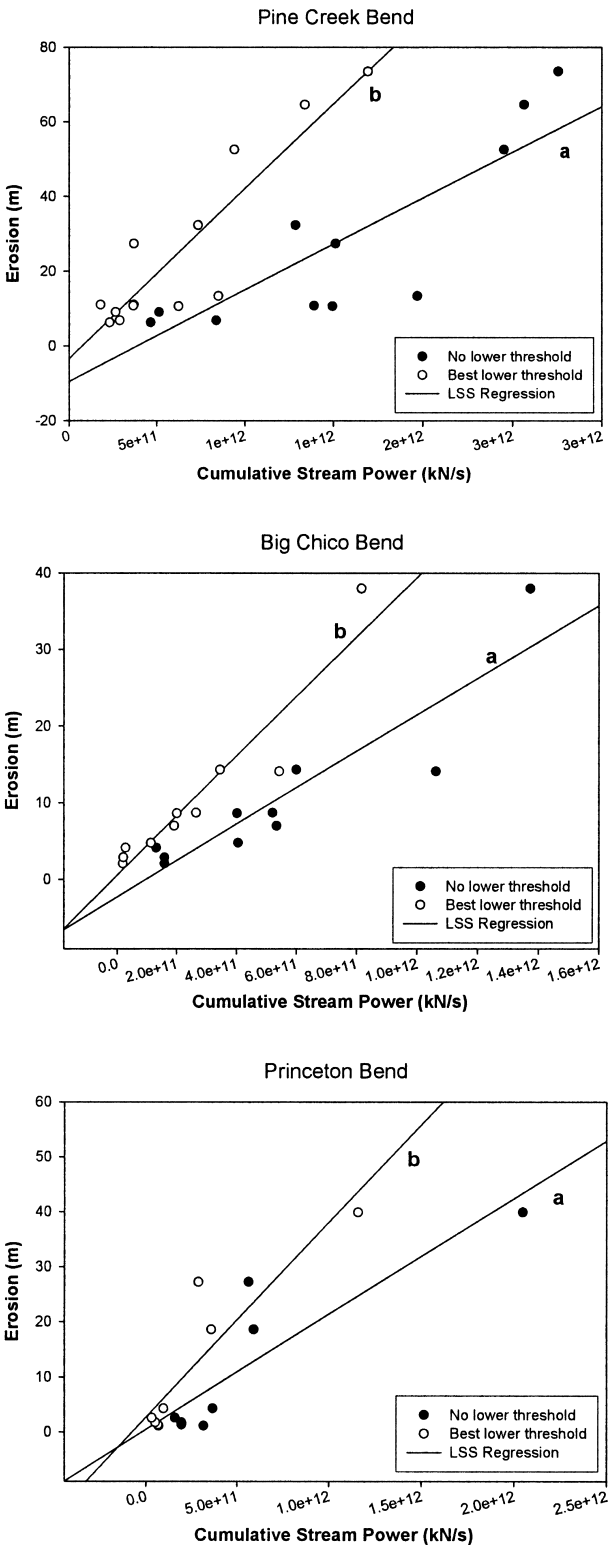

Figure 8. Three Figures Showing Two Regression Lines at Each Individual Site of Erosion Onto Stream Power: (a) the Full Circles are Stream Power Data Points Calculated Without a Lower Threshold (•); and (b) the Empty Circles Are Stream Power Values Calculated With the Best Performing Lower Threshold (o).

important to note that although the intercepts of the regression equation are reported in Table 3, only the regression of erosion onto all sites combined with a lower threshold had an intercept significantly different from zero at the 95 percent significance level.

Logarithmic transformation of the data at all sites combined produced a better distribution of points along both axes. The transformed equation shows an exponential relationship between stream power and discharge with an exponent less than one. This suggests that the influence of stream power on bank erosion is nonlinear, meaning that higher stream power events produced less erosion than predicted by a linear fit (Figures 10c and 10d).

Bank Erosion and Cumulative Discharge at Multiple Sites

Using the combined data from all sites, cumulative effective discharge (as opposed to cumulative effective stream power) was calculated to compare the relationship between discharge and erosion to that of stream power and erosion (see Figure 10). Stream power relationships are shown on the left-hand side and discharge relationships are shown on the right-hand side. Graphs of linear relationships are shown in the first row; graphs of log-log transformed data are shown in the second row. Relationships using stream power yielded more statistically significant results than those using discharge.

SUMMARY AND DISCUSSION

In this study, cumulative effective stream power correlated significantly with bank erosion. The regression relationships were highly significant ($r^2 > 0.70$) in each dataset tested, including the grouping of all the data. The relationships remained strong despite the fact that other predictor variables, such as bank material erodibility, channel curvature, bank height, and channel width, were not considered. As expected, the single-site regressions produced higher r-squared values than the combined datasets. Characteristics other than discharge are important for predicting the local magnitude of bank erosion and the spatial pattern of migration (for example: how migration is related to local channel curvature). However, our data suggest that cumulative effective stream power correlates with the magnitude of bank erosion between time intervals. The mean dimensionless bank erosion rate of 0.016 bankfull channel widths/yr [Table 2 (3.7 m/yr) (230 m)] was the same as the dimensionless

TABLE 3. Regression Results of Individual and Grouped Datasets. Threshold parameters and statistic for the three individual study sites (Pine Creek, Big Chico and Princeton) and two analyses of grouped data (three sites and all 13 sites).

Site		R/W	$Q_{threshold}$ (cms) (lower/upper)	r^2	p < (slope)	R-Ratio	N	p < (intercept)	Migration Equation (Ω_{ce} x 10^{-11})
Pine Creek	a	2.8	0 / none	0.70	0.0006	24	12	0.28	2.5 Ω_{ce} - 9.6
	b		310 / none	0.82	0.0001	45	12	0.70	6.0 Ω_{ce} - 0.3
	c		310 / 2,300	0.82	0.0001	45	12	0.70	5.4 Ω_{ce} - 2.1
Big Chico	a	2.9	0 / none	0.82	0.0003	37	10	0.41	2.4 Ω_{ce} - 2.2
	b		340 / none	0.90	0.0001	71	10	0.43	4.9 Ω_{ce} + 1.3
	c		340 / 2,800	0.91	0.0001	77	10	0.42	5.0 Ω_{ce} + 1.3
Princeton	a	2.0	0 / none	0.78	0.0037	21	8	0.91	2.1 Ω_{ce} + 0.5
	b		400 / none	0.83	0.0016	30	8	0.26	4.9 Ω_{ce} + 3.6
	c		400 / 2,300	0.83	0.0016	30	8	0.22	5.0 Ω_{ce} + 3.8
Combined 3	a	N/A	0 / none	0.75	0.0001	85	30	0.45	2.1 Ω_{ce} - 2.1
	b		340 / none	0.85	0.0001	156	30	0.52	5.5 Ω_{ce} + 1.2
Combined 13	a	N/A	0 / none	0.70	0.0001	152	66	0.12	1.3 Ω_{ce} + 3.1
	b		430 / none	0.71	0.0001	160	66	0.006	2.5 Ω_{ce} + 5.2

bank erosion rate on a range of 25 rivers that had a linear regression of 0.016 channel widths/yr (Larsen, 1995).

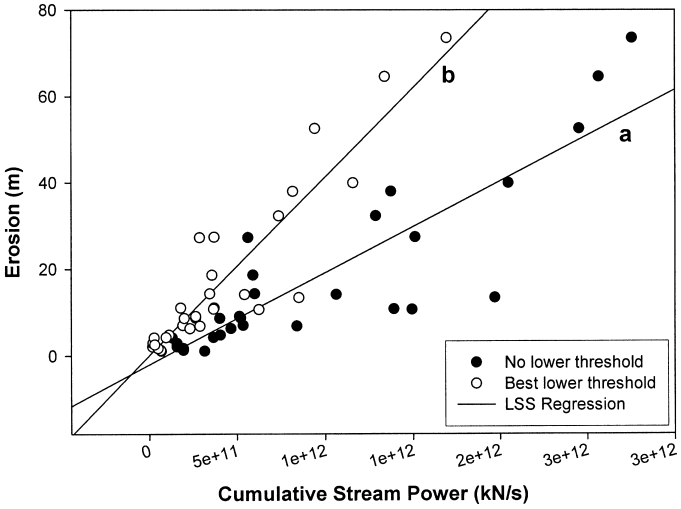

Figure 9. Shows Two Regression Lines of Erosion Onto Stream Power for the Combined Three Detailed Sites: (a) One Without a Lower Threshold (•); and (b) One With the Best Lower Threshold (o).

The regression between stream power and bank erosion probably does not express the entire relationship between flow rates and bank erosion rates. For example, flow duration may play a role. Although a linear relationship was used between cumulative effective stream power and erosion, there was a tendency, as evidenced by the power relationship with an exponent less than one, for higher discharges to have proportionally less effect (suggesting a nonlinear relationship).

Lower Threshold

Incorporating a lower threshold (i.e., a flow rate below which the stream power is assumed to not produce significant bank erosion) into stream power summations increases the accuracy of the regression relationship at the single-site level. The lower threshold values used for the regression analysis on the Sacramento River, which were all less than 430 m^3/s, eliminate most of the low (dry season) flows. These summer flows are known anecdotally not to produce significant channel migration (K. Buer, CDWR, 2004, personal communication). Thresholds below which significant bank erosion does not occur on the Sacramento River have been estimated at 1,200 to 1,700 m^3/s (K. Buer, CDWR, 2004, personal communication; CALFED, 2000). These previous estimates were based on qualitative observations, and may relate to discharge events that caused visible erosion of the bank. This study does not necessarily identify a physical lower threshold for erosion to occur, but does reveal that the relationship has greater statistical significance if a lower threshold is assumed.

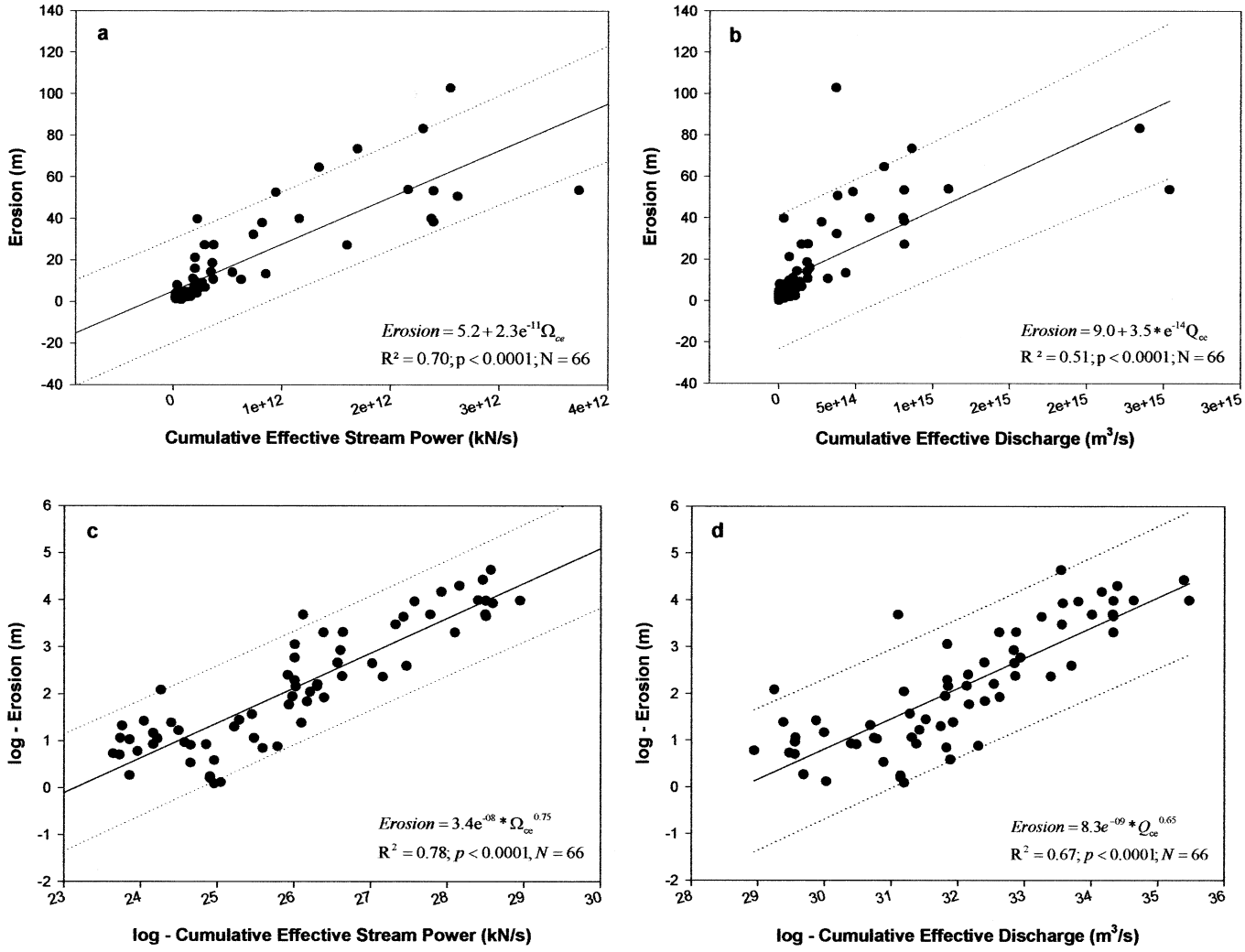

Figure 10. Regression Plots of Erosion and Cumulative Effective Stream Power and Discharge for All Sites Combined: (a) Plot of Erosion Onto Cumulative Effective Stream Power; (b) Plot of Erosion Onto Cumulative Effective Discharge; (c) Log-Log Plot of Erosion Onto Cumulative Effective Stream Power; and (d) Log-Log Plot of Erosion Onto Cumulative Effective Stream Power. Dotted lines indicate the 95 percent prediction interval.

The lower threshold identified in this analysis is considered below with respect to two different factors: (1) the frequency of discharges and (2) the sediment size at the toe of the bank. Together, lower flows over 62 years of records (< 450 m^3/s) have the highest cumulative volume because they are the most frequent (Figure 11). Removing low dry season flows from the stream power calculation, which are assumed not to cause significant migration, produce a better statistical relationship.

A lower threshold of significant bank erosion is most likely related to initiation of bank material movement, or to mechanical failure of the bank (ASCE, 1998). The capacity of a river to move sediment depends on the size of sediment being moved relative to the force available to move it. In many ways, stream power might be seen as a surrogate for bank shear stress. At stream powers lower than required to initiate sediment movement, bank erosion and meander migration theoretically cannot occur. Isolating this lower threshold has proven difficult because migration rates are controlled by several factors, including land cover (Brice, 1977; Micheli *et al.,* 2004), bend curvature, sediment transport rates, upstream planform shape, and cutbank heights (ASCE, 1998).

The lower threshold was determined based on statistical analysis rather than the analytical result of a physical process. To consider physical processes that could account for the lower flow threshold in bank erosion, a theoretical threshold was considered for particle movement of the bank. The average wall or bank shear stress τ_W (kg/ms^2) was estimated as a function of the average bed depth slope product (ASCE, 1998)

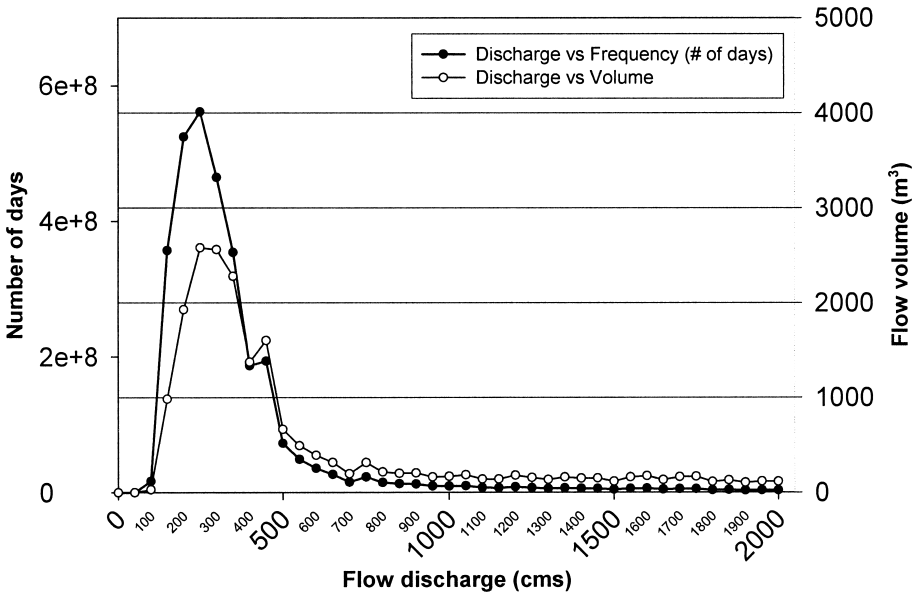

Figure 11. Flow Discharge Frequency Chart Illustrating the Distribution of Managed Flows Post-Shasta Dam. The high frequency of flows lower than 500 m^3/s is caused by mid-summer (dry season) water deliveries for agricultural use.

$$\overline{\tau_w} / \rho g H S = 0.7 \quad (5)$$

where ρg is the specific weight of water (γ, kg/m^2s^2), H is the average depth of the flowing water, and S (m/m) is the water surface slope. This relationship is based on empirical data for uniformly roughened trapezoidal channels. Field data were not available for this approximation. A bank slope of approximately 90 degrees was used, as the eroding banks on the Sacramento River sites are almost vertical, although a bank slope of 68 degrees would have given a very similar approximation (ASCE, 1998).

The depth slope product for the bed was estimated. Using average channel dimensions for a flow of 430 m^3/s (the lower threshold when all 13 sites were used), width 130 m, mean depth 2.9 m, mean velocity 1.15 m/s, and slope 0.0003 results in a Mannings' n of 0.031. The slope is an average of the tabulated slopes for the 13 sites, and the channel dimensions are estimates. Assuming the dimensionless Shield's number of 0.047 and using the D_{84} as the appropriate particle size (ASCE, 1998) for initial movement of a particle in the Shield's relationship,

$$\overline{\tau_w} / D_{84} (\rho_s - \rho_w) g = 0.047 \quad (6)$$

where ρ_s and ρ_w are the density of the sediment and water respectively, g is the gravitational constant, and D_{84} is the bank particle size of which 84 percent are finer), the bank shear stress for 430 m^3/s would initiate movement of an 8 mm particle.

Bank particle sizes at the toe of the bank for the 13 sites were estimated from the closest sites in a report by Water Engineering and Technology, Inc. (1988). The mean and median D_{84} bank particle sizes (of the 13 sites) were 13 and 14 mm, respectively, with a standard deviation of 14 (Table 2). Excluding one high value of 45 mm resulted in mean and median values of 10 and 12 mm, respectively, with a standard deviation of 8 mm.

The data and analyses show that the bank or wall particle size that can be mobilized by the bank shear stress of the lower threshold flow is similar to the mean average and median D_{84} particle of the toe of the bank (of these sites). This suggests that the lower threshold flow may be related to the initiation of motion of the toe of the bank. Even when such initial motion and bank scour does occur, higher flows may be required to evacuate the collected material.

Analysis at Multiple Sites. When all 13 datasets were combined and regressed against cumulative effective stream power, using a lower threshold did not improve the relationship. This is most likely because the erosion/stream power relationship is obscured by other factors influencing bank erosion, such as channel curvature and bank material. Losing the effect of the lower threshold when other factors are not held constant suggests that those factors have a greater effect on migration rate than excluding flows with lower stream powers. However, because a lower threshold improves the relationship at the site scale, it suggests that lower flows should be excluded.

If the lower threshold relates to the initiation of bank material movement, site specific thresholds may be able to be related to site specific factors such as bank sediment size. However, our data did not produce a clear relationship between sites, probably because bank material sizes were estimated from nearby sites. More precise bank material data would

allow more thorough research into the relationship between the lower threshold and bank material size. This finding warrants further study of what flows are required to initiate motion of the bank material.

Upper Threshold and the Influence of Individual Events

Using an upper threshold (i.e., excluding overbank flows from the relationship) did result in a better relationship, albeit very slight. The use of an upper threshold was excluded because the influence was not significantly large; however, there is evidence that on some systems, bank erosion is greater at magnitudes allowing overbank flows. On the Carson River, Carroll *et al.* (2004) found that bank erosion was significantly greater at flows above bankfull.

The relationship between flow magnitude and bank erosion varies in different river types. Some rivers maintain a quasi-stable width over decades or centuries. Such systems can increase their width due to high magnitude flood flows, but the width is subsequently restored following years of more normal flows (ASCE, 1998). Historical data from 1904 to 1997 show that the Sacramento River is undergoing a process of progressive bank migration accompanied by point bar growth on the opposite bank, a process that maintains a quasi-stable equilibrium width (Wolman, 1959; Leopold *et al.,* 1964; Leopold, 1994). In some systems where the width is conserved, the highest flows are not responsible for the most erosion (Wolman, 1959; Leopold *et al.,* 1964; Leopold, 1994) and the equilibrium width can even survive a flood. The Sacramento River, in our study reach, approximates such a quasi-equilibrium system. In contrast, the Carson River experienced maximum bank erosion in response to flood flows, with 87 percent of the mass eroded over a six-year period occurring in a single flood (Carroll *et al.,* 2004). Rivers in semi-arid regions of the Western USA are known to vary in width in response to flood events (ASCE, 1998), and the Carson may be an example of this. Because bank erosion processes occur in a variety of geomorphic, geologic, and climatic contexts, results from one type of river may not be applicable in other contexts.

The results of log transformation suggest that the relationship between stream power and bank erosion is nonlinear. As stream power increases, its correlation with bank erosion drops below a linear fit. This power relationship, with an exponent less than one, suggests that the effects of higher discharges on bank erosion on the Sacramento River dissipate as waters spread over the floodplain. In doing so, they no longer add a proportionate amount of force to the cutbank.

A nonlinear relationship in our analysis may remain hidden because each data point represents the cumulative migration between time intervals, not discrete flow events. Figure 12 presents a conceptual relationship between cumulative stream power and bank erosion. At low cumulative stream power values, erosion does not increase appreciably due to the lack of sediment initiation. After this threshold is passed, erosion increases at a relatively linear rate until flow begins to spread over the banks. At this point, the erosion rate drops below linear. The form of this relationship (Figure 12) is related to channel properties such as curvature, bank material, and the cross sectional shape of the channel and floodplain. The linear relationship found in our study approximates the central part of the conceptual curve in Figure 12.

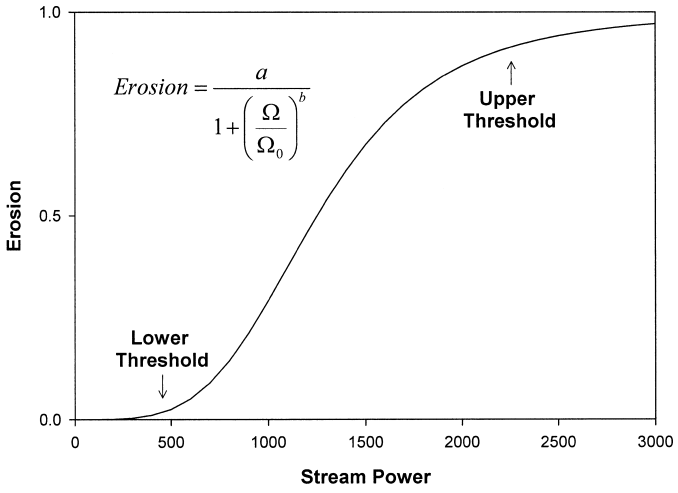

Figure 12. The Curve Illustrates a Theoretical Relationship Between Erosion and Stream Power Where Low and High Values of Stream Power Do Not Significantly Affect the Amount of Bank Erosion. The parameter a is the midpoint value on the stream power axis, b is the slope of the logistic curve, and Ω_0 is the maximum amount of erosion.

Tributary Influences

Although it has been suggested that bends at or just downstream from stream tributary confluences migrate faster due to sediment input (Constantine *et al.,* 2004), our data do not show this pattern. Princeton and Packer Island, which (along with Pine Creek) have the highest mean average erosion rates, are not located near confluences. Bank erosion data from Pine Creek, which had the highest rate of bank erosion, were measured just upstream from the confluence with Pine Creek. The M&T bend is at the direct confluence with a tributary, yet it has not migrated significantly in the past 100 years. However, the Big

Chico bend is just downstream of the confluence with Big Chico Creek, beyond the M&T site. This bend does have a higher migration rate compared to the other bends surveyed. Similar migration rates at sites close to each other, Pine Creek/Big Chico and Packer Island/Princeton, suggest that there may be a spatial component (perhaps related to bank material) to erosion rate.

Implications for Channel Migration Modeling

Although many components control bank erosion rates, this study focused on flow. The strong regression relationship between cumulative effective stream power and bank erosion suggests flow is the dominant influence in controlling bank erosion rates. This has great implications for channel meander migration models that use constant flow rates to simulate migration (e.g., Howard, 1992). The idea that bank erosion can be related to stream power has been conceptually incorporated into a meander migration model in the companion paper (Larsen *et al.,* 2006a).

Many current mechanistic models of channel migration depend primarily on the instream velocity patterns to predict the distance and direction of bank migration (e.g., Ikeda *et al.,* 1981; Johannesson and Parker, 1989; Nelson and Smith, 1989; Howard, 1992; Mosselman, 1998; Sun *et al.,* 2001; Darby *et al.,* 2002). Some models of bank migration assume that a single continuous discharge occurs, and that the banks erode continuously in response. This approach is based on the working model of "bankfull discharge." Many migration models have used a characteristic discharge to model the velocity in the channel. This constant discharge is used over the entire time of prediction. Models that assume bank erosion is proportional to the near bank velocity use a constant discharge to calibrate an erosion coefficient (Micheli and Larsen, 1997; Micheli *et al.,* 2004;). Then, the same discharge is used to develop a modeled velocity that is applied in the model predictions (Larsen *et al.,* 2006a).

A constant discharge that represents the integrated cumulative effect of a range of discharges is most valuable when bank migration is considered over an extended period of time. After 50 to 100 years, the calibrated linked system of velocity and erosion coefficient can be used to predict long term migration (Larsen *et al.,* 2006a). While this is useful in long term predictions, other applications, which have shorter time periods or changing flow patterns, will benefit from more realistic, variable flow values.

Stream power can be used to represent the effects of time varying flow in a migration model that has the ability to account for the other effects such as bank erodibility (Larsen and Greco, 2002), curvature (Larsen *et al.,* 2002), and other factors. For example, in systems where the flow is highly variable, such as semi-arid and arid regions, incorporating the effects of variable flow may vastly increase the utility of meander migration models. Incorporating the effects of variable flow can also improve the analysis of flow regulation scenarios and water diversions. The companion paper (Larsen *et al.,* 2006a) illustrates how this can be done.

Implications for Vegetation Modeling

Connecting hydrogeomorphic models with patterns of vegetation will help investigators understand the potential impacts of altering the flow regime and floodplain (Auble *et al.,* 1994; Larsen *et al.,* 2006a, Larsen *et al.,* 2006b). Longer periods of time (> one year) are necessary to analyze patterns of change in highly erratic systems. To model this variability, it is necessary to capture how variable flow patterns create a dynamic and heterogeneous landscape through flooding and channel migration. The stream power relationship described here offers a method to incorporate a variable flow component into a meander migration model (see Larsen *et al.,* 2006b). This permits spatial modeling of floodplain development and vegetation change that considers the stochastic nature of the hydrology. This is important considering the episodic recruitment of primary successional species such as cottonwood (*Populus* sp.). Representing the timing of floodplain deposition more realistically permits a reference community to be analyzed in more detail. This information, in turn, should improve restoration design strategies. Variation in flow creates the new floodplain land and vegetation patches over time. These dynamic flows are essential for maintaining the functional integrity (i.e., quality) of many floodplain habitats and the populations of biota dependent upon them (Naiman *et al.,* 1993; Scott *et al.,* 1996; Greco *et al.,* 2002).

APPENDIX A
BANK EROSION AND CUMULATIVE EFFECTIVE STREAM POWER DATA

	Migration Distance (m)	Cumulative Effective Stream Power (kgm/s^3) (no lower threshold)	Cumulative Effective Stream Power (kgm/s^3) (with threshold)	Beginning Date	Ending Date	Number of Days	Migration Rate (m/year)
Big Chico	0.501949	2.12E+06	601800	6/15/1988	12/15/1988	183	1.001
Big Chico	0.958544	3.99E+06	884824	12/15/1988	5/15/1989	151	2.317
Big Chico	0.248367	1.87E+06	300697	5/15/1989	6/15/1990	396	0.229
Big Chico	4.141727	1.52E+06	320390	6/15/1990	1/15/1991	214	7.064
Big Chico	2.075891	1.84E+06	214359	1/15/1991	8/15/1991	212	3.574
Big Chico	2.878679	1.84E+06	235179	8/15/1991	4/15/1992	244	4.306
Big Chico	6.990578	6.19E+06	2.22E+06	4/15/1992	8/15/1993	487	5.239
Big Chico	14.09488	1.23E+07	6.29E+06	8/15/1993	8/15/1995	730	7.047
Big Chico	8.623161	4.66E+06	2.32E+06	8/15/1995	5/15/1996	274	11.487
Big Chico	14.29643	6.95E+06	4.00E+06	5/15/1996	4/15/1997	335	15.577
Big Chico	37.96249	1.59E+07	9.45E+06	4/15/1997	4/15/1999	730	18.981
Big Chico	8.689936	6.03E+06	3.07E+06	4/15/1999	3/15/2000	335	9.468
Big Chico	4.785537	4.70E+06	1.31E+06	3/15/2000	4/15/2001	396	4.411
Coyote Creek	0.292495	1.53E+06	332350	6/15/1988	11/15/1988	153	0.698
Coyote Creek	0.982998	1.49E+06	210970	11/15/1988	5/15/1989	181	1.982
Coyote Creek	0.172743	2.04E+06	366620	5/15/1989	12/15/1989	214	0.295
Coyote Creek	0.123637	1.27E+06	82900	12/15/1989	6/15/1990	182	0.248
Coyote Creek	0.163598	1.55E+06	123250	6/15/1990	1/15/1991	214	0.279
Coyote Creek	0.007227	979420	35130	1/15/1991	6/15/1991	151	0.017
Coyote Creek	0.425459	2.08E+06	150740	6/15/1991	4/15/1992	305	0.509
Coyote Creek	0.180259	1.43E+06	130	4/15/1992	11/15/1992	214	0.307
Coyote Creek	2.324163	3.70E+06	1.51E+06	11/15/1992	8/15/1993	273	3.107
Coyote Creek	27.20418	3.88E+07	1.85E+07	8/15/1993	5/15/2000	2465	4.028
Fosters Island	6.70E-05	2.09E+06	575801	6/15/1988	12/15/1988	183	0.000
Fosters Island	0.114925	1.49E+06	305848	12/15/1988	5/15/1989	151	0.278
Fosters Island	0	3.92E+06	839743	5/15/1989	6/15/1990	396	0.000
Fosters Island	0.017947	1.84E+06	283116	6/15/1990	1/15/1991	214	0.031
Fosters Island	0.124532	1.48E+06	141827	1/15/1991	7/15/1991	181	0.251
Fosters Island	0	2.37E+06	282379	7/15/1991	5/15/1992	305	0.000
Fosters Island	0.142642	1.47E+06	25811.8	5/15/1992	11/15/1992	184	0.283
Fosters Island	5.849319	4.39E+06	2.12E+06	11/15/1992	8/15/1993	273	7.821
Fosters Island	53.93317	4.64E+07	2.50E+07	8/15/1993	6/15/2000	2496	7.887
Fosters Island	1.221319	3.30E+06	759724	6/15/2000	4/15/2001	304	1.466
Hartley's 1	0.008591	887791	95756.6	8/15/1986	11/15/1986	92	0.034
Hartley's 1	0.0029	2.26E+06	759874	11/15/1986	5/15/1987	181	0.006
Hartley's 1	0.006756	1.89E+06	604383	5/15/1987	11/15/1987	184	0.013
Hartley's 1	0.046465	1.92E+06	329802	11/15/1987	6/15/1988	213	0.080
Hartley's 1	0.063427	1.72E+06	65909.8	6/15/1988	11/15/1988	153	0.151
Hartley's 1	3.203769	1.84E+06	361730	11/15/1988	6/15/1990	577	2.027
Hartley's 1	2.488502	2.26E+06	587913	6/15/1990	1/15/1991	214	4.244
Hartley's 1	2.886703	5.94E+06	1.35E+06	1/15/1991	10/15/1991	273	3.860
Hartley's 1	1.304655	2.38E+06	265853	10/15/1991	4/15/1992	183	2.602

APPENDIX A (cont'd.)
BANK EROSION AND CUMULATIVE EFFECTIVE STREAM POWER DATA

	Migration Distance (m)	Cumulative Effective Stream Power (kgm/s^3) (no lower threshold)	Cumulative Effective Stream Power (kgm/s^3) (with threshold)	Beginning Date	Ending Date	Number of Days	Migration Rate (m/year)
Hartley's 1	2.018151	1.40E+06	232935	4/15/1992	11/5/1992	204	3.611
Hartley's 1	21.17752	4.63E+06	2.29E+06	11/5/1992	8/15/1993	283	27.314
Hartley's 1	53.36474	5.22E+07	2.77E+07	8/15/1993	5/15/2001	2830	6.883
Hartley's 2	0.094279	1.89E+06	604383	6/15/1988	11/15/1988	153	0.225
Hartley's 2	0.800608	5.94E+06	1.35E+06	11/15/1988	6/15/1990	577	0.506
Hartley's 2	0.021486	1.92E+06	329802	6/15/1990	1/15/1991	214	0.037
Hartley's 2	0	2.18E+06	265853	1/15/1991	9/15/1991	243	0.000
Hartley's 2	0.541349	1.60E+06	232935	9/15/1991	4/15/1992	213	0.928
Hartley's 2	0.022247	1.77E+06	65909.8	4/15/1992	11/15/1992	214	0.038
Hartley's 2	3.992152	5.82E+06	2.50E+06	11/15/1992	12/15/1993	395	3.689
Hartley's 2	40.01524	5.09E+07	2.75E+07	12/15/1993	5/15/2001	2708	5.393
Larkin's 1	0	887791	95756.6	8/15/1986	11/15/1986	92	0.000
Larkin's 1	0	1.84E+06	361730	11/15/1986	5/15/1987	181	0.000
Larkin's 1	0	2.26E+06	759874	5/15/1987	11/15/1987	184	0.000
Larkin's 1	0.448323	2.26E+06	587913	11/15/1987	6/15/1988	213	0.768
Larkin's 1	0	1.89E+06	604383	6/15/1988	11/15/1988	153	0.000
Larkin's 1	0.617015	2.28E+06	545507	11/15/1988	6/15/1989	212	1.062
Larkin's 1	0.41467	3.66E+06	801471	6/15/1989	6/15/1990	365	0.415
Larkin's 1	0.031852	1.92E+06	329802	6/15/1990	1/15/1991	214	0.054
Larkin's 1	0.218573	2.38E+06	265853	1/15/1991	10/15/1991	273	0.292
Larkin's 1	0.885864	1.40E+06	232935	10/15/1991	4/15/1992	183	1.767
Larkin's 1	0.252082	1.77E+06	65909.8	4/15/1992	11/15/1992	214	0.430
Larkin's 1	9.844808	4.58E+06	2.29E+06	11/15/1992	8/15/1993	273	13.162
Larkin's 1	38.40526	5.22E+07	2.77E+07	8/15/1993	5/15/2001	2830	4.953
MandT	0.236927	1.36E+07	7.24E+06	5/15/1995	5/15/1997	731	0.118
MandT	0	1.65E+07	9.75E+06	5/15/1997	6/15/1999	761	0.000
MandT	0.2506	958578	409578	6/15/1999	8/15/1999	61	1.499
MandT	0.015851	4.39E+06	2.41E+06	8/15/1999	3/28/2000	226	0.026
MandT	0.552855	4.47E+06	1.20E+06	3/28/2000	4/15/2001	383	0.527
Ord Bend	0	1.51E+06	168806	8/15/1986	1/15/1987	153	0.000
Ord Bend	0.182875	1.38E+06	399392	1/15/1987	5/15/1987	120	0.556
Ord Bend	0.295346	2.40E+06	872391	5/15/1987	11/15/1987	184	0.586
Ord Bend	0.474203	1.98E+06	545550	11/15/1987	5/15/1988	182	0.951
Ord Bend	0.776057	2.73E+06	892897	5/15/1988	12/15/1988	214	1.324
Ord Bend	0.337759	1.66E+06	406811	12/15/1988	5/15/1989	151	0.816
Ord Bend	0.021422	4.34E+06	1.14E+06	5/15/1989	6/15/1990	396	0.020
Ord Bend	0.037659	2.04E+06	399583	6/15/1990	1/15/1991	214	0.064
Ord Bend	0.992549	2.01E+06	324851	1/15/1991	8/15/1991	212	1.709
Ord Bend	0.785678	2.01E+06	294904	8/15/1991	4/15/1992	244	1.175
Ord Bend	0.116749	1.88E+06	132939	4/15/1992	11/15/1992	214	0.199
Ord Bend	7.698904	5.91E+06	2.80E+06	11/15/1992	11/15/1993	365	7.699
Ord Bend	50.67319	5.40E+07	3.03E+07	11/15/1993	4/15/2001	2708	6.830

APPENDIX A (cont'd.)
BANK EROSION AND CUMULATIVE EFFECTIVE STREAM POWER DATA

	Migration Distance (m)	Cumulative Effective Stream Power (kgm/s^3) (no lower threshold)	Cumulative Effective Stream Power (kgm/s^3) (with threshold)	Beginning Date	Ending Date	Number of Days	Migration Rate (m/year)
Pine Creek	73.48082	3.19E+07	1.96E+07	9/7/1937	6/6/1942	1733	15.476
Pine Creek	27.36788	1.75E+07	4.29E+06	6/6/1942	6/13/1947	1833	5.450
Pine Creek	10.74293	1.61E+07	4.25E+06	6/13/1947	7/18/1951	1496	2.621
Pine Creek	9.055522	5.95E+06	3.08E+06	7/18/1951	6/26/1952	344	9.608
Pine Creek	13.37027	2.28E+07	9.85E+06	6/26/1952	9/10/1956	1537	3.175
Pine Creek	52.53983	2.84E+07	1.09E+07	9/10/1956	6/25/1962	2114	9.071
Pine Creek	6.824652	9.71E+06	3.36E+06	6/25/1962	6/23/1964	729	3.417
Pine Creek	6.264746	5.39E+06	2.69E+06	6/23/1964	5/15/1965	326	7.014
Pine Creek	10.61981	1.73E+07	7.23E+06	5/15/1965	6/7/1968	1119	3.464
Pine Creek	32.26976	1.49E+07	8.52E+06	6/7/1968	5/20/1970	712	16.543
Pine Creek	64.56416	2.97E+07	1.55E+07	5/20/1970	9/25/1974	1589	14.831
Pine Creek	11.02719	4.29E+06	2.09E+06	9/25/1974	5/27/1975	244	16.496
Packer Island	0.778319	2.18E+06	645591	6/15/1988	12/15/1988	183	1.552
Packer Island	0.42031	1.92E+06	329802	12/15/1988	6/15/1989	182	0.843
Packer Island	0.121955	1.53E+06	58034.1	6/15/1989	6/15/1990	365	0.122
Packer Island	3.385677	2.00E+06	504299	6/15/1990	1/15/1991	214	5.775
Packer Island	1.794561	3.66E+06	801471	1/15/1991	10/15/1991	273	2.399
Packer Island	2.793025	2.38E+06	265853	10/15/1991	5/15/1992	213	4.786
Packer Island	3.751255	1.64E+06	240811	5/15/1992	11/15/1992	184	7.441
Packer Island	15.91085	4.58E+06	2.29E+06	11/15/1992	8/15/1993	273	21.273
Packer Island	83.31041	4.79E+07	2.66E+07	8/15/1993	5/15/2000	2465	12.336
Princeton	2.528839	1.84E+06	361730	11/15/1986	5/15/1987	181	5.100
Princeton	1.273934	2.26E+06	759874	5/15/1987	11/15/1987	184	2.527
Princeton	1.702806	2.26E+06	587913	11/15/1987	6/15/1988	213	2.918
Princeton	0.378892	2.18E+06	645591	6/15/1988	12/15/1988	183	0.756
Princeton	0.198359	2.00E+06	504299	12/15/1988	6/15/1989	182	0.398
Princeton	1.091316	3.66E+06	801471	6/15/1989	6/15/1990	365	1.091
Princeton	0	1.92E+06	329802	6/15/1990	1/15/1991	214	0.000
Princeton	0.985403	2.38E+06	265853	1/15/1991	10/15/1991	273	1.317
Princeton	0.173769	1.64E+06	240811	10/15/1991	5/15/1992	213	0.298
Princeton	0.002875	1.53E+06	58034.1	5/15/1992	11/15/1992	184	0.006
Princeton	96.9379	1.54E+07	7.96E+06	11/15/1992	5/15/1995	911	38.839
Princeton	27.25093	6.51E+06	3.33E+06	5/15/1995	5/15/1996	366	27.176
Princeton	18.61036	6.84E+06	4.15E+06	5/15/1996	3/15/1997	304	22.345
Princeton	39.90784	2.37E+07	1.34E+07	3/15/1997	5/15/2000	1157	12.590
Princeton	4.230486	4.24E+06	1.11E+06	5/15/2000	5/15/2001	365	4.230
Rancho de Farwell	0	1.51E+06	168806	8/15/1986	1/15/1987	153	0.000
Rancho de Farwell	0.169386	2.43E+06	842269	1/15/1987	5/15/1987	120	0.515
Rancho de Farwell	0.396296	4.34E+06	1.14E+06	5/15/1987	11/15/1987	184	0.786
Rancho de Farwell	0.07039	2.04E+06	399583	11/15/1987	5/15/1988	182	0.141
Rancho de Farwell	0.103918	2.01E+06	324851	5/15/1988	11/15/1988	184	0.206
Rancho de Farwell	0.21607	1.88E+06	132939	11/15/1988	5/15/1989	181	0.436

APPENDIX A (cont'd.)
BANK EROSION AND CUMULATIVE EFFECTIVE STREAM POWER DATA

	Migration Distance (m)	Cumulative Effective Stream Power (kgm/s^3) (no lower threshold)	Cumulative Effective Stream Power (kgm/s^3) (with threshold)	Beginning Date	Ending Date	Number of Days	Migration Rate (m/year)
Rancho de Farwell	0.843055	3.65E+06	1.00E+06	5/15/1989	6/15/1990	396	0.777
Rancho de Farwell	8.014577	1.38E+06	399392	6/15/1990	1/15/1991	214	13.670
Rancho de Farwell	1.122814	2.40E+06	872391	1/15/1991	8/15/1991	212	1.933
Rancho de Farwell	2.620254	1.98E+06	545550	8/15/1991	4/15/1992	244	3.920
Rancho de Farwell	4.001973	1.95E+06	457439	4/15/1992	11/15/1992	214	6.826
Rancho de Farwell	2.176686	2.01E+06	294904	11/15/1992	8/15/1993	273	2.910
Rancho de Farwell	39.7299	4.86E+06	2.55E+06	8/15/1993	6/15/2000	2496	5.810
Rancho de Jimeno	0.215198	2.43E+06	1.07E+06	6/15/1988	11/15/1988	153	0.513
Rancho de Jimeno	0.86642	4.69E+06	1.58E+06	11/15/1988	6/15/1989	212	1.492
Rancho de Jimeno	0.235588	2.46E+06	665471	6/15/1989	6/15/1990	365	0.236
Rancho de Jimeno	0.324308	2.27E+06	444115	6/15/1990	1/15/1991	214	0.553
Rancho de Jimeno	3.659794	2.92E+06	1.04E+06	1/15/1991	10/15/1991	273	4.893
Rancho de Jimeno	2.516315	3.05E+06	721802	10/15/1991	4/15/1992	183	5.019
Rancho de Jimeno	2.852411	1.80E+06	382011	4/15/1992	11/15/1992	214	4.865
Rancho de Jimeno	53.64787	6.79E+07	4.32E+07	11/15/1992	6/15/2000	2769	7.072
Rancho de Jimeno	2.407821	4.83E+06	1.83E+06	6/15/2000	5/15/2001	334	2.631

ACKNOWLEDGMENTS

The authors would like to thank Koll Buer, Stacy Cepello, and Adam Henderson of the California Department of Water Resources for the bank erosion data, and for their continued help. The authors also would like to thank the anonymous reviewers for their insightful comments, along with Alex Young. This research was sponsored by the California Department of Water Resources, Northern District under SAP Contract Number 4600002133. Thanks to HKR.

LITERATURE CITED

ASCE (American Society of Civil Engineers), 1998. River Width Adjustment. I: Processes and Mechanisms. Journal of Hydraulic Engineering, pp. 881-902.

Auble, G.T., J.M. Friedman, and M.L. Scott, 1994. Relating Riparian Vegetation to Present and Future Streamflows. Ecological Applications 4(3): 544-554.

AutoDesk, 2004. AutoCAD Software. Autodesk Inc., San Rafael, California.

Bagnold, R.A., 1960. Some Aspects of the Shape of River Meanders. U.S. Geological Survey Professional Paper 282-E, pp. 135-144.

Begin, Z.B., 1981. Stream Curvature and Bank Erosion. Journal of Geology 89:497-504.

Brice, J., 1977. Lateral Migration of the Middle Sacramento River, California. USDI Geological Survey Water Res. Investigations 77-43, 51 pp.

Buer, K., D. Forwalter, M. Kissel, and B. Stohler, 1989. The Middle Sacramento River: Human Impacts on Physical and Ecological Processes Along a Meandering River. USDA Forest Service, General Technical Report.

CALFED, 2000. Final Programmatic Environmental Impact Statement/Environmental Impact Report. CALFED Bay-Delta Program, Sacramento, California.

CDWR (California Department of Water Resources), 1994. Sacramento River Bank Erosion Investigation Memorandum Progress Report. State of California, The Resources Agency, Department of Water Resources, Northern District.

CDWR (California Department of Water Resources), 1995. Memorandum Report: Sacramento River Meander Belt Future Erosion Investigation. CDWR 155, The Resources Agency, Department of Water Resources, Sacramento, California.

CALWATER, 1997. CALWATER (Version 2.2): The California Watershed Map. The California Interagency Watershed Mapping Committee, California Resources Agency, Sacramento, California.

Carroll, R.W.H., J.J. Warwick, A.I. James, and J.R. Miller, 2004. Modeling Erosion and Overbank Deposition During Extreme Flood Conditions on the Carson River, Nevada. Journal of Hydrology 297(1-4):1-21.

Constantine, C.R., T. Dunne, and M.B. Singer, 2004. Controls on Migration Rates in the Sacramento River and Implications for Improving Prediction of Meander Migration. Third Biennial CALFED Bay-Delta Program Science Conference, Sacramento, California, USA, pp. 44.

Darby, S.E. and C.R. Thorne, 1996. Development and Testing of Riverbank-Stability Analysis. Journal of Hydraulic Engineering 122(8):443-454.

Darby, S.E., A.M. Alabyan, and M.J. Van de Wiel, 2002. Numerical Simulation of Bank Erosion and Channel Migration in Meandering Rivers. Water Resources Research 38(9):1163.

ESRI (Environmental Systems Research Institute), 2003. ArcGIS 8.3. Environmental Systems Research Institute, Redlands, California.

Fremier, A.K., 2003. Floodplain Age Modeling Techniques to Analyze Channel Migration and Vegetation Patch Dynamics on the Sacramento River, California. Masters Thesis, University of California, Davis, California, 97 pp.

Gergel, S.E., M.D. Dixon, and M.G. Turner, 2002. Consequences of Human-Altered Floods: Levees, Floods, and Floodplain Forests Along the Wisconsin River. Ecological Applications 12(6):1755-1770.

Golet, G.H., D.L. Brown, E.E. Crone, G.R. Geupel, S.E. Greco, K.D. Holl, D.E. Jukkola, G.M. Kondolf, E.W. Larsen, F.K. Ligon, R.A. Luster, M.P. Marchetti, B.K. Nur, B.K. Orr, D.R. Peterson, M.E. Power, W.E. Rainey, M.D. Roberts, J.G. Silveira, S.L. Small, J.C. Vick, D.S. Wilson, and D.M. Wood, 2003. Using Science to Evaluate Restoration Efforts and Ecosystem Health on the Sacramento River Project, California. *In:* California Riparian Systems: Processes and Floodplain Management, Ecology, and Restoration, P.M. Faber (Editor). Riparian Habitat and Floodplains Conference Proceedings, Riparian Habitat Joint Venture, Sacramento, California, pp. 368-385.

Greco, S.E. and C.A. Alford, 2003. Historical Channel Mapping From Aerial Photography of the Sacramento River, Colusa to Red Bluff, California: 1937 to 1997. Technical Report Prepared for California Department of Water Resources, Northern District, Red Bluff, California, Landscape Analysis and Systems Research Laboratory, Department of Environmental Design, University of California, Davis, California, 101 pp.

Greco, S.E. and R.E. Plant, 2003. Temporal Mapping of Riparian Landscape Change on the Sacramento River, Miles 196-218, California, USA. Landscape Research 28:405-426.

Greco, S.E., R.E. Plant, and R.H. Barrett, 2002. Geographic Modeling of Temporal Variability in Habitat Quality of the Yellow-Billed Cuckoo on the Sacramento River, Miles 196-219, California. *In:* Predicting Species Occurrences: Issues of Accuracy and Scale, J.M. Scott, P.J. Heglund, F. Samson, J. Haufler, M. Morrison, M. Raphael, and B. Wall (Editors). Island Press, Covelo, California, pp. 183-196.

Greco, S.E., J.L. Tuil, and A. Wheaton, 2003. A Historical Aerial Photography Collection of the Sacramento River From Colusa to Red Bluff: 1937-1998. Technical Report Prepared for the California Department of Water Resources, Northern District, Red Bluff, California, Landscape Analysis and Systems Research Laboratory, Department of Environmental Design, University of California, Davis, California.

Hasegawa, K., 1989. Universal Bank Erosion Coefficient for Meandering Rivers. Journal of Hydraulic Engineering 115:744-765.

Hickin, E.J. and G.C. Nanson, 1984. Lateral Migration Rates of River Bends. Journal of Hydraulic Engineering 110(11):1557-1567.

Howard, A.D., 1992. Modeling Channel Migration and Floodplain Sedimentation in Meandering Streams. *In:* Lowland Floodplain Rivers, P.A. Carling and G.E. Petts (Editors). Geomorphological Perspectives. John Wiley and Sons, New York, New York, 1-41.

Hupp, C.R. and W.R. Osterkamp, 1996. Riparian Vegetation and Fluvial Geomorphic Processes. Geomorphology 14(4):277-295.

Ikeda, S., G. Parker, and K. Sawai, 1981. Bend Theory of River Meanders. Part 1. Linear Development. Journal of Fluid Mechanics 112:363-377.

Johannesson, H. and G. Parker, 1989. Linear Theory of River Meanders. *In:* River Meandering, S. Ikeda and G. Parker (Editors). American Geophysical Union, Washington, D.C.

Knighton, D., 1998. Fluvial Forms & Processes: A New Perspective. John Wiley and Sons, New York, New York, 383 pp.

Larsen, E.W., 1995. The Mechanics and Modeling of River Meander Migration. PhD Dissertation., University of California, Berkeley, California.

Larsen, Eric W., Alexander K. Fremier, and Evan H. Girvetz, 2006a. Modeling the Effects of Variable Annual Flow on River Channel Meander Migration Patterns, Sacramento River, California, USA. Journal of American Water Resources Association (JAWRA) 42(4):1063-1075.

Larsen, E.W., E. Anderson, E. Avery, and K. Dole, 2002. The Controls on and Evolution of Channel Morphology of the Sacramento River: A Case Study of River Miles 201-185. The Nature Conservancy, Chico, California.

Larsen, E.W., E.H. Girvetz, and A.K. Fremier, 2006b. Assessing the Effects of Alternative Setback Levee Scenarios Employing a River Meander Migration Model. Environmental Management 37(6):880-897

Larsen, E.W. and S.E. Greco, 2002. Modeling Channel Management Impacts on River Migration: A Case Study of Woodson Bridge State Recreation Area, Sacramento River, California, USA. Environmental Management 30(2):209-224.

Leopold, L.B., 1994. A View of the River (First Edition). Harvard University Press, Cambridge, Massachusetts.

Leopold, L.B., M.G. Wolman, and J.P. Miller, 1964. Fluvial Processes in Geomorphology. W. H. Freeman and Company, San Francisco, California, 522 pp.

Mahoney, J.M. and S.B. Rood, 1998. Streamflow Requirements for Cottonwood Seedling Recruitment – An Integrative Model. Wetlands 18(4):634-645.

Malanson, G.P., 1993. Riparian Landscapes. Cambridge University Press, Cambridge, Massachusetts.

Micheli, E.R., J.W. Kirchner, and E.W. Larsen, 2004. Quantifying the Effect of Riparian Forest Versus Agricultural Vegetation on River Meander Migration Rates, Central Sacramento River, California, USA. River Research and Applications 20(5):537-548.

Micheli, E.R. and E.W. Larsen, 1997. Bank Erosion and Meander Migration Rates of the Upper Sacramento River. EOS Transactions, AGU 78(46):256-256.

Mosselman, E., 1998. Morphological Modeling of Rivers With Erodible Banks. Hydrological Processes 12:1357-1370.

Naiman, R.J., H. Décamps, and M. Pollock, 1993. The Role of Riparian Corridors in Maintaining Regional Biodiversity. Ecological Applications 3(2):209-212.

Nanson, G.C. and E.J. Hickin, 1986. A Statistical Analysis of Bank Erosion and Channel Migration in Western Canada. Geological Society of America Bulletin 97:497-504.

Nelson, J.M. and J.D. Smith, 1989. Flow in Meandering Channels With Natural Topography. *In:* River Meandering, S. Ikeda and G. Parker (Editors). American Geophysical Union, Water Resources Monograph 12, Washington, D.C., pp. 69-102.

Osman, A.M. and Thorne, C.R., 1988. Riverbank Stability Analysis: I: Theory. Journal of Hydraulic Engineering, 114, No. 2: 134-150.

Pizzuto, J.E. and T.S. Meckelenburg, 1989. Evaluation of a Linear Bank Erosion Equation. Water Resources Research 5:1005-1013.

Richter, B.D. and H.E. Richter, 2000. Prescribing Flood Regimes to Sustain Riparian Ecosystems Along Meandering Rivers. Conservation Biology 14(5):1467-1478.

Scott, M.L., J.M. Friedman, and G.T. Auble, 1996. Fluvial Process and the Establishment of Bottomland Trees. Geomorphology 14:327-339.

Sklar, L.S. and W.E. Dietrich, 2004. A Mechanistic Model for River Incision Into Bedrock by Saltating Bed Load. Water Resources Research 40:W06301.

Sun, T., P. Meakin, and T. Jossang, 2001. A Computer Model for Meandering Rivers With Multiple Bed Load Sediment Sizes. 1. Theory. Water Resources Research 37(8):2227-2241.

Tabacchi, E., D.L. Correll, R. Hauer, G. Pinay, A.M. Planty-Tabacchi, and R.C. Wissmar. 1998. Development, Maintenance and Role of Riparian Vegetation in the River Landscape. Freshwater Biology 40:497-516.

USACE (U.S. Army Corps of Engineers), 2002. HEC-RAS River Analysis System. U.S. Army Corps of Engineers, Hydrologic Engineering Center, Davis, California.

USGS (U.S. Geological Survey), 2004. USGS Stream Flow Discharge. *Available at* http://water.usgs.gov/nwis/sw.

Water Engineering and Technology, Inc., 1988. Geomorphic Analysis of the Sacramento River. Draft Report, DACWO5-87-C-0084, Water Engineering and Technology, Inc., U.S. Army Corps of Engineers, Sacramento, California.

Wolman, M.G., 1959. Factors Influencing Erosion of a Cohesive River Bank. Am. Jour. Sci. 257:204-216.